Journal of the European Ceramic Society 19 (1999) 463–468

PII: S0955-2219(98)00213-1
0955-2219/99/$—see front matter

Pressureless Sintering of Al_2O_3/Ni Nanocomposites

R. Z. Chen and W. H. Tuan*

Institute of Materials Science and Engineering, National Taiwan University, Taipei, 10764 Taiwan

(Received 2 May 1998; revised version received 20 August 1998; accepted 30 August 1998)

Abstract

In the present study, an Al_2O_3/Ni nanocomposite containing 5 vol% Ni is prepared by pressureless sintering at 1400°C for 2 h. Most nickel inclusions, around 70% in the sintered nanocomposite, locate at the intergranular sites, the triple junctions and Al_2O_3/Al_2O_3 grain boundaries. The average size of the nickel inclusions at the triple junctions, grain boundaries and intragranular locations is 145, 131 and 73 nm, respectively. The average size of all nickel inclusions is 118 nm. The presence of nickel inclusions can prohibit the grain growth of matrix grains. The size of Al_2O_3 grains in the sintered nanocomposite is only 490 nm. The strength of the nanocomposite is thus high for the refined microstructure. The matrix Al_2O_3 grains and Ni inclusions at triple junctions underwent considerable coarsening during a post-annealing treatment at 1300°C for 2 h. The strength of the annealed composites is thus reduced significantly after annealing. © *1999 Elsevier Science Limited. All rights reserved*

Keywords: sintering, Al_2O_3, strength, microstructure-final, nanocomposites.

1 Introduction

More and more evidence highlights that the strength of ceramics can be significantly enhanced by adding nano-sized ceramic or metallic inclusions.[1–5] The size of the so-called nano-sized inclusions is in the range of 100 nm or smaller than 100 nm.[1] The composite containing the nano-sized inclusions is coined by Roy as nanocomposite.[6] Among the nanocomposites investigated, the Al_2O_3/SiC system has attracted much attention. Three strengthening mechanisms were proposed for the system. These mechanisms are (1) flaw size reduction,[1,2] (2) grinding effect[4,5] and (3) grain boundary strengthening effect.[7] The first mechanism suggested that the strength of the nanocomposites is enhanced for the size of flaws is drastically reduced.[12] This mechanism also related the strengthening to the formation of dislocation networks.[1] The dislocations could form subgrain boundaries after a post-annealing treatment, the strength could thus be further enhanced. The second mechanism related the strengthening to the introduction of a compressive surface stress during abrasive grinding.[4,5] The compressive stress in the nanocomposite was not relived after a post-annealing treatment; however, the surface cracks generated during grinding were healed.[8] The strength of the nanocomposite was thus further enhanced after the annealing treatment. Differ to the fracture mode for monolithic alumina, the fracture mode for the nanocomposite was mainly transgranular. On the basis of this observation, the third mechanism suggested that the strength increase was contributed by the grain boundary strengthening.[7]

The above mentioned strengthening mechanisms are all based on the fact that the thermal expansion coefficient of Al_2O_3 and SiC is different. By choosing a system with reverse thermal properties offers an opportunity to examine the strengthening mechanism for nanocomposite. In the present study, Al_2O_3/Ni nanocomposite are prepared. Unlike the Al_2O_3/SiC system, the thermal expansion coefficient of the nano-sized phase, Ni, is higher than that of the matrix, Al_2O_3.

The microstructure of the nanocomposite can play an important role on the strengthening effect. Furthermore, the size as well as the locations, intergranular site or transgranular site, of the inclusions may also affect the strength of the nanocomposite. However, the microstructure of the metal-strengthened nanocomposites is more difficult to be controlled than that of the ceramic-strengthened

*To whom correspondence should be addressed. Fax: +886-2-2363-4562; e-mail:tuan@ccms.ntu.edu.tw

nanocomposite.[9] It mainly due to the metals are usually in their molten state during sintering as the melting point of metals is usually low. The diffusion rate in liquid phase is more rapid than that in solid phase. Furthermore, the wetting of molten metal on ceramic is usually poor. The coarsening of the molten metallic particles in ceramic matrix is thus much faster than that of solid ceramic particles in ceramic matrix.[9,10] Therefore, most metal-strengthened nanocomposites are prepared by hot-pressing technique.[3,9] This technique allows the nanocomposites to be densified at a relatively low temperature; the coarsening of metallic inclusions is thus suppressed. For example, Sekino et al had applied hot-pressing technique to prepare Ni-strengthened Al_2O_3.[3] The size of the resulting Ni inclusions is as small as 96 nm; the strength of the nanocomposite can be as high as 1·6 times that of alumina alone.

The processing of nanocomposite is also a challenging task. For the Al_2O_3/SiC nanocomposites, the strength enhancement can only be found in the hot-pressed specimens but not in the pressureless sintered nanocomposite.[11] However, the hot-pressing technique may impose limit on the application of nanocomposites for the cost reason. In the present study, processing techniques to prepare nickel-strengthened nanocomposite by pressureless sintering are explored. Furthermore, the microstructure of the nanocomposite is carefully analyzed. The strengthening mechanism for the nanocomposite is also investigated.

2 Experimental

An alumina powder (TM-DR, Taimei Chem. Co. Ltd., Japan) and nickel nitrate powder (Johnson Matthey Co., USA) were mixed and stirred in water at 30°C for 24 h. The amount of nickel nitrate was controlled to result in 5 vol% Ni in the composite after sintering. The water was then removed by drying on a heating pad. The residue was washed with distilled water twice and dried in an oven for 24 h. The dried lumps were crushed and passed through a 150 mesh plastic sieve. The powder was then reduced in a dry hydrogen at 500°C for 12 h. The reduced powder was milled again in ethyl alcohol for 4 h to break the agglomerates. The slurry was then dried with a rotary evaporator and sieved. Powder compacts were formed by pressing uniaxially at 56 MPa. The specimens were then arranged within a covered graphite crucible. The use of graphite crucible could generate an atmosphere of carbon monoxide, CO, during sintering.[12] Sintering was taken place at 1400°C for 2 h. The heating and cooling rates were 5°C min^{-1}. The fired specimens were then ground longitudinally with a diamond wheel. The final size of the ground specimens was $4 \times 3 \times 40$ mm. Some ground specimens were further annealed in the graphite crucible at 1300°C for 2 h. The monolithic alumina specimens were prepared with the same procedures for those of composites.

The phases analysis was performed by X-ray diffractometry (XRD). The apparent density of the sintered specimens was determined by the water displacement method. The flexural strength and fracture toughness were determined respectively by the 4-point bending technique and the single-edge-notched beam technique. The rate of loading was 0·5 mm min^{-1}. The microstructure was observed by scanning electron microscopy (SEM) and transmission electron microscopy (TEM). The size of Al_2O_3 and Ni inclusions was measured with the TEM micrographs.

3 Results

The XRD analysis reveals only Al_2O_3 and Ni phases in the powder after reduction in dry hydrogen, (Fig. 1) The phases remain the same after sintering and after post-annealing. Figure 2 shows the morphology of Al_2O_3 particles and Al_2O_3/Ni powder mixtures. The size of Al_2O_3 particles is around 200 nm; the shape is irregular. Fine Ni particles, around 20 nm, are observed on the surface of alumina particles; the shape is roughly spherical.

Typical TEM micrographs of Al_2O_3 and Al_2O_3/Ni composites after sintering are shown in Fig. 3 The relative density of the specimens is shown in Table 1, the size of Ni inclusions shown in Table 2. The average size of all Ni particles is 118 nm. Therefore, the Al_2O_3/Ni composite prepared in the present study fulfills the definition of nanocomposite. Most nickel inclusions seat at the intergranular sites, i.e., the Al_2O_3/Al_2O_3 grain

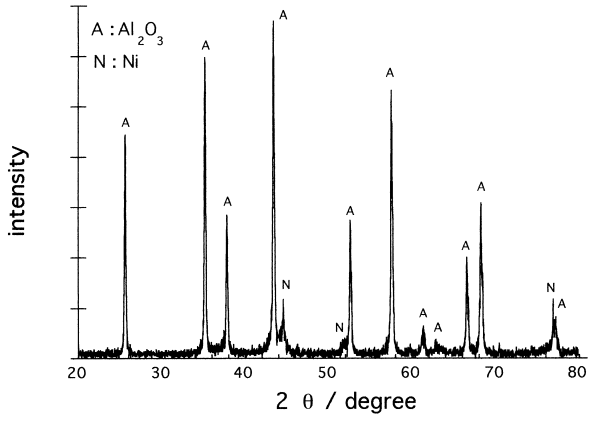

Fig. 1. The XRD pattern for the Al_2O_3/Ni powder mixtures after reduction in hydrogen at 500°C for 12 h.

boundaries or the triple junctions, [Fig. 3(b)]. There are around 1/3 of the nickel inclusions are located within the Al_2O_3 grains. The size distribution of nickel inclusions is shown in Fig. 4 The nickel inclusions seated at the triple junction is slightly larger than that of the nickel inclusions seated between two matrix grains. The intragranular nickel inclusions are the smallest. The strength and toughness of the sintered specimens are shown in Table 1. The strength of alumina is increased by 35% as nano-sized nickel inclusions are added; the toughness increased by 20%.

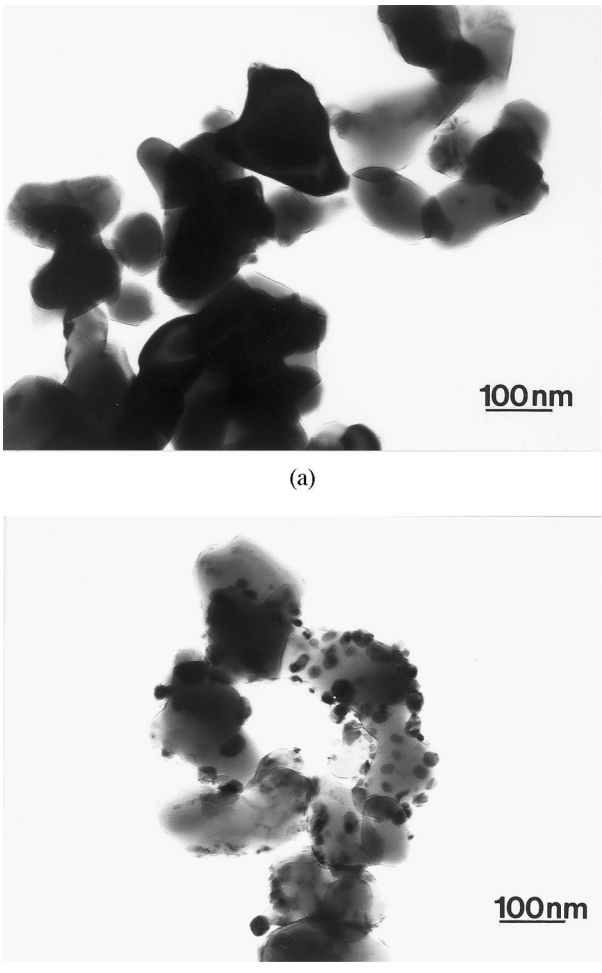

(a)

(b)

Fig. 2. TEM micrographs of (a) Al_2O_3 and (b) Al_2O_3/Ni powder mixtures.

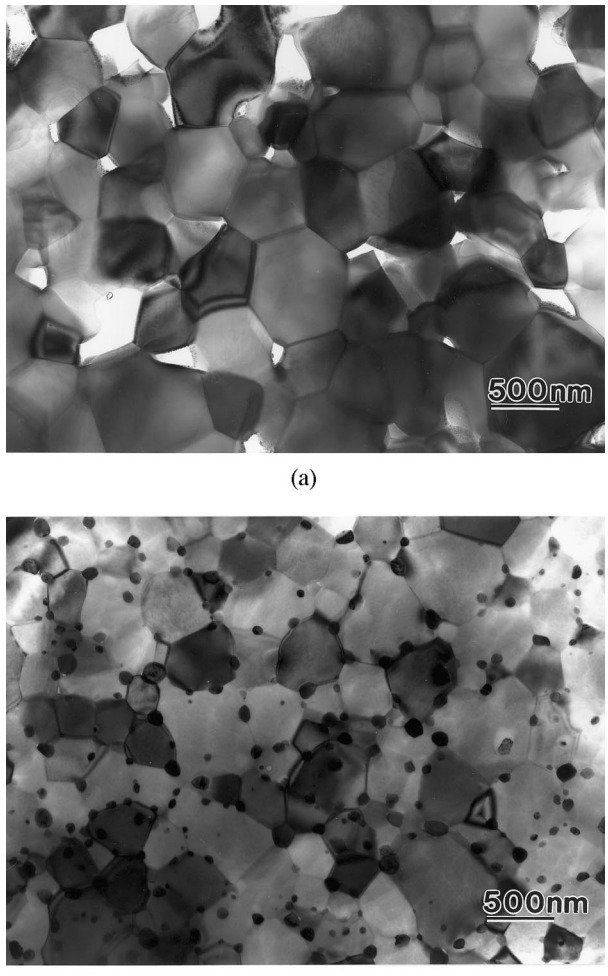

(a)

(b)

Fig. 3. Typical TEM micrographs of sintered (a) Al_2O_3 and (b) Al_2O_3/Ni nanocomposite.

Table 1. The density, flexural strength and fracture toughness of the sintered and annealed Al_2O_3 and Al_2O_3/Ni nanocomposites

		Relative density (%)	*Size of Al_2O_3 matrix (nm)*	*Strength (MPa)*	*Toughness ($MPam^{0.5}$)*
Sintered	Al_2O_3	93·9 ± 0·5	750 ± 65	390 ± 45	3·6 ± 0·1
	Al_2O_3/Ni	96·6 ± 0·5	490 ± 60	526 ± 37	4·2 ± 0·1
Annealed	Al_2O_3	94·0 ± 0·7	1402 ± 410	357 ± 48	4·9 ± 0·2
	Al_2O_3/Ni	96·7 ± 0·4	933 ± 134	386 ± 46	5·4 ± 0·2

Table 2. The size of Ni inclusions in the sintered and annealed Al_2O_3/Ni nanocomposites

		At the triple junctions	*On the Al_2O_3/Al_2O_3 grain boundaries*	*Within the Al_2O_3 grains*	*All Ni inclusions*
Sintered	Amount (%)	30	36	34	100
	Sixe (nm)	145 ± 42	131 ± 50	73 ± 30	118 ± 51
Annealed	Amount (%)	44	34	22	100
	Size (nm)	329 ± 147	164 ± 83	92 ± 43	219 ± 148

The relative density, the size of Al_2O_3 grains and Ni inclusions of annealed specimens are also shown in Tables 1 and 2. Typical micrographs of the Al_2O_3 and Al_2O_3/Ni composite after the post-annealing treatment are shown in Fig. 5. The distribution of the nickel inclusions in the annealed specimens is shown in Fig. 6. Both Al_2O_3 grains and Ni inclusions underwent considerable coarsening during annealing. The strength of the Al_2O_3 and Al_2O_3/Ni composite is thus significantly reduced after annealing, (Table 2).

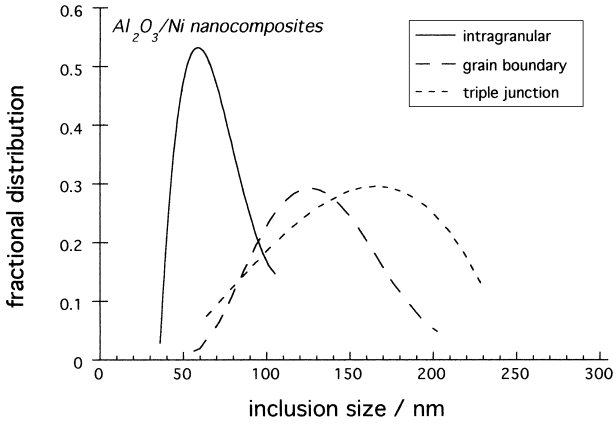

Fig. 4. The size distribution of Ni inclusions at intragranular sites, grain boundaries and triple junctions in the sintered Al_2O_3/Ni nanocomposite.

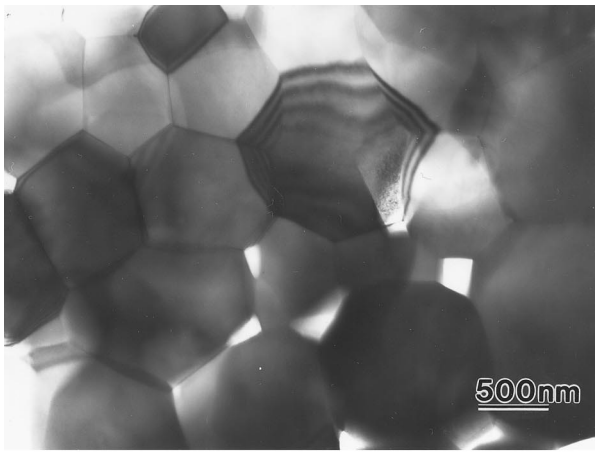

(a)

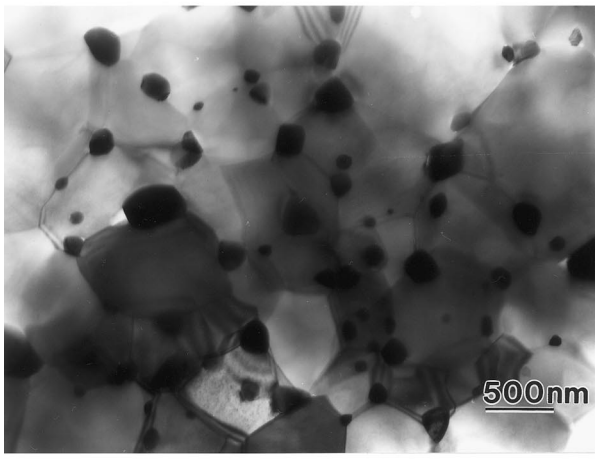

(b)

Fig. 5. Typical TEM micrographs of post-annealed (a) Al_2O_3 and (b) Al_2O_3/Ni nanocomposite.

4 Discussion

Since the coarsening of molten metallic inclusions in ceramic matrix is fast,[9,10] the sintering temperature used in the present study is lower than the melting point of nickel to avoid the problem. However, the solid nickel inclusions still underwent considerable coarsening, from 20 to around 100 nm. The Al_2O_3 matrix grains are also grown from around 200 to 490 nm after sintering. The movement of Al_2O_3 grain boundaries can bring along the Ni inclusions; the solid Ni inclusions are thus coarsened. Furthermore, the size of Al_2O_3 grains in the nanocomposite is smaller than that in the monolithic Al_2O_3, (Table 1). It indicates that the presence of nickel inclusions slows down the movement of the grain boundaries of Al_2O_3. Due to the refined microstructure of the nanocomposite, the density of the nanocomposite is higher than that of monolithic alumina, (Table 1). The grain growth behaviour of the Ni-strengthened Al_2O_3 may be similar to that of a porous Al_2O_3. The separation between grain boundary and inclusion can take place as the velocity of the grain boundary is much faster that of inclusion.[13] Figures 4 and 6 indicate that the Ni inclusions with the size smaller than 100 nm can be separated from the grain boundaries of Al_2O_3. It implies that 100 nm is the critical size for Ni inclusions. If the size of all Ni inclusions can be smaller than 100 nm, most Ni inclusions can then be swallowed by Al_2O_3 grains.

The sintering temperature used in the present study is as low as 1400°C, the relative density of Al_2O_3/Ni nanocomposite is thus only 96·6%. The

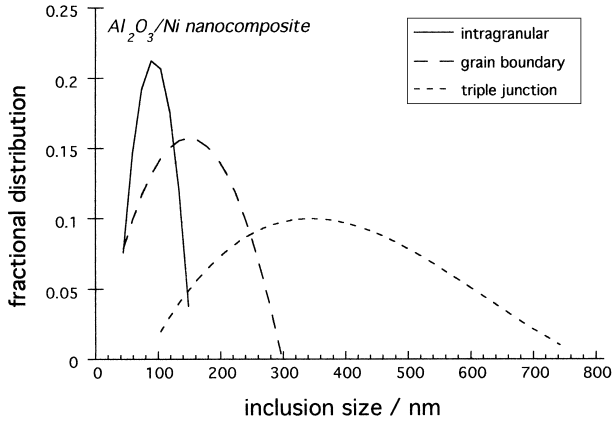

Fig. 6. The size distribution of Ni inclusions at intragranular sites, grain boundaries and triple junctions in the post-annealed Al_2O_3/Ni nanocomposite.

increase of sintering temperature can increase final density; however, the increase of sintering temperature can also enlarge the size of Ni inclusions.[10] Furthermore, the coarsening of Ni particles can be very rapid above the melting point of Ni, 1453°C. The sintering temperature, 1400°C, can thus be taken as the maximum temperature allowable to prepare the Al_2O_3/Ni nanocomposite. The strength of ceramics depends strongly on the amount of porosity. The strength of Al_2O_3/Ni nanocomposite can be further enhanced if the amount of porosity is low. It is indeed found by Sekino et al on their hot-pressed Al_2O_3/Ni nanocomposite.[3]

Figures 4 and 6 indicate that the Ni inclusions at triple junctions are significantly coarsened after annealing. Table 1 shows that the size of Al_2O_3 grains in the annealed Al_2O_3 and Al_2O_3/Ni composite is almost 2 times that in the sintered specimens. The growth of triple-junction inclusions is accompanied by the coarsening of matrix grains. The growth of grain-boundary inclusions is slow for the diffusion coefficient of Ni ion along the grain boundaries of Al_2O_3 is very small ($\delta D_b = 7{\cdot}0 \times 10^{-21}\ m^3 s^{-1} at 1400°C$; δ is the grain boundary thickness, D_b the grain-boundary diffusivity).[14] The diffusion coefficient of Ni ion in Al_2O_3 lattice is expected even smaller; the coarsening of intragranular Ni inclusions is thus not significant after the post-annealing treatment.

The strength of sintered and annealed Al_2O_3 and Al_2O_3/Ni composites is shown as a function of the size of Al_2O_3 grains in Fig. 7. A linear relationship is exhibited. It indicates that the strength of the nanocomposite depends strongly on the matrix grain size. The strengthening effect for Al_2O_3/Ni nanocomposite is thus contributed by microstructural refinement. The fracture surfaces of monolithic Al_2O_3 and Al_2O_3/Ni composite are shown in Fig. 8. There is no significant difference between the fracture mode of the monolithic Al_2O_3 and the Al_2O_3/Ni nanocomposites. The grain boundary strengthening mechanism is thus not active in the present system. The strength of Al_2O_3/Ni nanocomposite is reduced by 25% after the annealing at 1300°C for 2 h. The annealing condition used in the present study is the same as that used for the Al_2O_3/SiC nanocomposites. However, the microstructure coarsening during annealing is not reported in the Al_2O_3/SiC system. It may due to the atmosphere used during annealing is different. The thermal expansion of the inclusion is larger than that of matrix in the present system. The strengthening mechanisms induced by the thermal expansion mismatch between Al_2O_3/SiC system are not likely observed in the Al_2O_3/Ni system. However, the presence of second phase, independent of ceramic or metallic phase, can prohibit the grain growth of matrix grains. It implies that the most important strengthening mechanism for nanocomposite is microstructural refinement. To refine the microstructure, the processing conditions should be carefully controlled. However, the driving force for the grain growth of the refined microstructure is high. The microstructure is therefore sensitive to the post heat treatment.

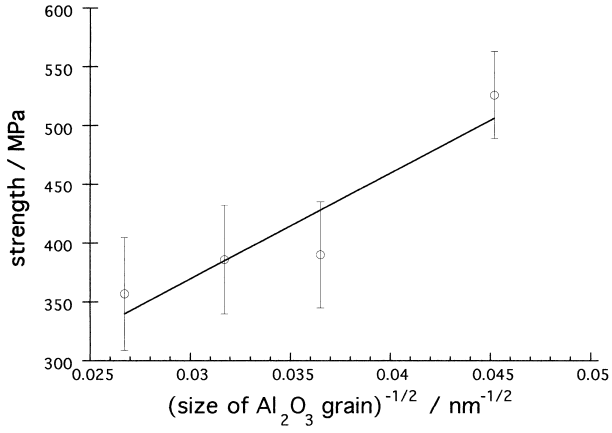

Fig. 7. The strength of sintered and annealed Al_2O_3 and Al_2O_3/Ni specimens as a function of Al_2O_3 grain size.

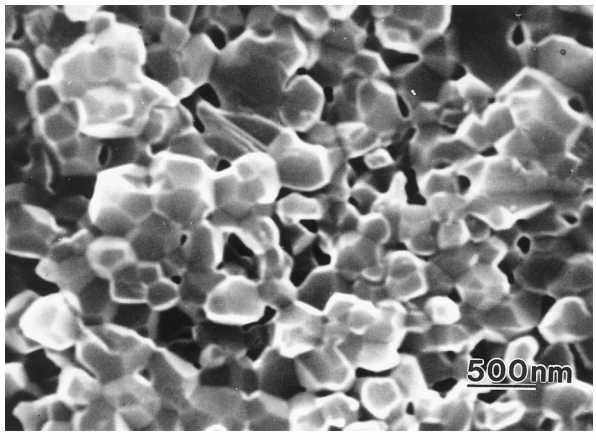

(a)

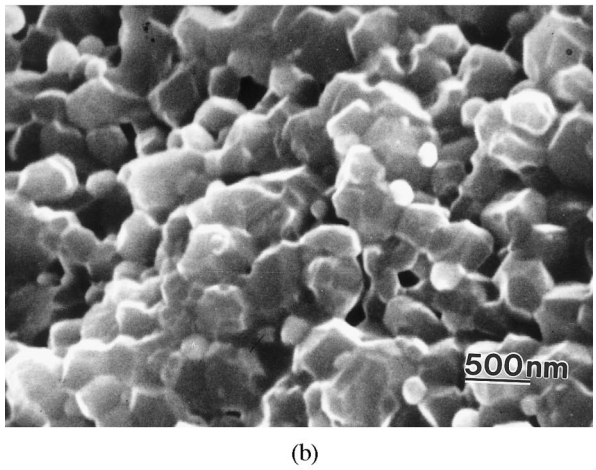

(b)

Fig. 8. The fracture surfaces of the sintered (a) Al_2O_3 and (b) Al_2O_3/Ni nanocomposite.

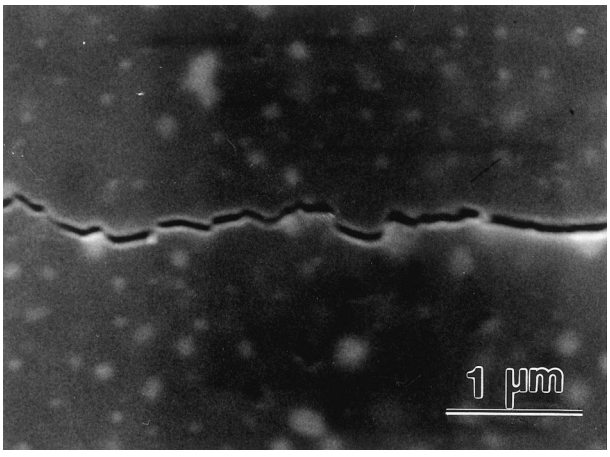

Fig. 9. The interactions between a crack introduced by indentation and Ni inclusions in the sintered Al_2O_3/Ni nanocomposite.

Similar to the results for the composites containing micro-sized inclusions,[10,14] the toughness of alumina is also enhanced due to the presence of nano-sized inclusions. The toughness enhancement is contributed from the toughening agent acting either on the crack path or in front of crack tip. For the Al_2O_3/SiC nanocomposite, the contribution from the interactions between crack path and SiC particles is ignored for the size of SiC particles is too small to bridge the crack surfaces.[11] However, the bridging Ni particles can be found on the crack path, Fig. 9 It mainly due to the ductility of Ni is better than that of SiC. The crack surfaces can still be bridged by the nano-sized Ni inclusions, the toughness of Al_2O_3 is thus enhanced.

5 Conclusions

The processing conditions to prepare Al_2O_3/Ni nanocomposite by pressureless sintering are explored. The microstructure of the nanocomposite is carefully analyzed. Most the nickel inclusions locate at the boundary and triple junction sites. The Ni inclusions with the size smaller than 100 nm can be separated from the grain boundaries of Al_2O_3. The lattice diffusion coefficient of Ni ion in Al_2O_3 is expected to be low, the coarsening of the intragranular Ni inclusions is thus slow in the subsequent heat treatment. However, The size of matrix Al_2O_3 grains and the Ni inclusions at triple junctions is significantly enlarged after annealing at 1300°C for 2 h. It indicates that not only the size but also the location of nano-sized phase are critical for the microstructure of nanocomposite. The strengthening of the nanocomposite is attributed to microstructural refinement. The strength of the Al_2O_3/Ni composite is thus dropped after annealing. Due to the ductility of Ni, the presence of nano-sized Ni inclusions can also enhance the toughness of Al_2O_3.

References

1. Niihara, K., New design concept of structural ceramic–ceramic nanocomposites. *J. Ceram. Soc. Jpn.*, 1991, **99**, 974–982.
2. Borsa, C. E., Jiao, S., Todd, R. I. and Brook, R. J., Processing and properties of Al_2O_3/SiC nanocomposites. *J. Microscopy*, 1994, **177**, 305–312.
3. Sekino, T., Nakajima, T., Ueda, S. and Niihara, K., Reduction and sintering of a nickel–dispersed–alumina composite and its properties. *J. Am. Ceram. Soc.*, 1997, **80**, 1139–1148.
4. Zhao, J., Stearns, L. C., Harmer, H. P., Chan, H. M., Miller, G. A. and Cook, R. E., Mechanical behavior of alumina–silicon carbide nanocomposite. *J. Am. Ceram. Soc.*, 1993, **76**, 503–510.
5. Chou, I. A., Chan, H. M. and Harmer, M. P., Machining-induced surface residual stress behaviour in Al_2O_3-SiC nanocomposites. *J. Am. Ceram. Soc.*, 1996, **79**, 2403–2409.
6. Roy, R., Roy, R. A. and Roy, D. M., Alternative perspectives on quasi-crystallinity: non-uniformity and nanocomposites. *Mater. Lett.*, 1986, **4**, 323–328.
7. Jiao, S., Jenkins, M. L. and Davidge, R. W., Interfacial fracture energy-mechanical behaviour relationship in Al_2O_3/SiC and Al_2O_3/TiN nanocomposites. *Acta Mater.*, 1997, **45**, 149–156.
8. Thompson, A. M., Chan, H. M., Harmer, M. P. and Cook, R. E., Crack healing and stress relaxation in Al_2O_3–SiC nanocomposites. *J. Am. Ceram. Soc.*, 1995, **78**, 567–571.
9. Oh, S-T., Sekino, T. and Niihara, K., Fabrication and mechanical properties of 5 vol% copper dispersed alumina nanocomposite. *Journal of the European Ceramic Society*, 1998, **18**, 31–37.
10. Tuan, W. H., Wu, H. H. and Yang, T. J., The preparation of Al_2O_3/Ni composites by a powder coating technique. *J. Mater. Sci.*, 1995, **30**, 855–859.
11. Sternitzke, M., Review: structural ceramic nanocomposites. *Journal of the European Ceramic Society*, 1997, **17**, 1061–1082.
12. Tuan, W. H. and Brook, R. J., The toughening of alumina with nickel inclusions. *Journal of the European Ceramic Society*, 1990, **6**, 31–37.
13. Brook, R. J., Controlled grain growth. In *Ceramic Fabrication Processes, Treatise on Materials Science and Technology*, 1976, ed. F. F. Y. Wang. Academic Press, New York, 1976, pp. 331–364.
14. Kaur, I., Gust, W. and Kozma, L., In *Handbook of Grain and Interphase Boundary Diffusion Data*, Vol. 1. Ziegler Press, Stuttgart, 1989, pp. 222–223.